Available online at www.sciencedirect.com

ScienceDirect

IFAC PapersOnLine 56-2 (2023) 2456–2461

Design of Sliding Mode Controller based on Radial Basis Function Neural Network for Spacecraft Autonomous Proximity

Jianfang Jia*, Yongjun Wang*, Hong Yue**

**School of Electrical and Control Engineering, North University of China, Taiyuan 030051, China (e-mail: jiajianfang@nuc.edu.cn, 5460714@qq.com).*
***Department of Electronic and Electrical Engineering, University of Strathclyde, Glasgow G11XW, UK (e-mail: hong.yue@strath.ac.uk).*

Abstract: Since the dynamic model of spacecraft has the characteristics of non-linear, kinematic couplings, uncertainties and nonstationary disturbance, it has become a challenging problem to accurately control the relative position and attitude of the spacecraft. A radial basis function neural network (RBFNN)-based sliding mode controller (SMC) is proposed for trajectory tracking of spacecraft autonomous proximity in this paper. Firstly, a six degree-of-freedom (DOF) relative motion dynamics model is developed for close proximity operations. The modified Rodrigues parameters are applied to solve the problem of singularity. Then, a SMC that does not require accurate model information is designed. RBFNN is used to adaptively eliminated the model uncertainty impacts on the system. Finally, the stability of the relative motion dynamics is proved via Lyapunov stability theory. Simulation results illustrate that the method can attenuate the attitude and position errors, reduce the chattering of the input and decrease the overshoot of the control torque effectively.

Copyright © 2023 The Authors. This is an open access article under the CC BY-NC-ND license (https://creativecommons.org/licenses/by-nc-nd/4.0/)

Keywords: Spacecraft, relative motion, sliding mode control, neural network, Lyapunov stability

1. INTRODUCTION

The spacecraft usually carries flexible attachments such as robotic arms and antennas to fix the special mission. However, the spacecraft is subject to various environmental disturbance forces and torques, such as solar radiation pressure, gravity gradient, and the Earth's magnetic field while on orbit. Therefore, it is difficult to apply classical linear system control methods to solve the attitude orbit coupling problem between the chaser and target spacecraft.

Many researches focus on applications of neural networks in modeling of unknown functions in dynamical control systems (Narendra et al., 1990; Levin et al., 1996; Lewis et al., 1998; Ge et al., 2010). These methods show that a variety of unknown nonlinearities and external disturbances for the spacecraft control system can be solved using neural networks. Considering the vibration problem in the attitude tracking process of flexible spacecraft, an adaptive multi-layer neural network control method was used to approximate external interference in (Kong et al., 2011). Yuan et al. (2019) designed an attitude tracking robust controller, and the RBFNN is introduced to approximate the model uncertainty, but it was only adopted in spacecraft attitude control, did not discuss 6-DOF coupling control. Wang et al. (2015) proposed a controller where a RBFNN is utilized to adaptively learn the uncertainty bound in the Lyapunov sense and thus the uncertainty effects are effectively eliminated.

SMC applies a high-speed switching control law to drive the system states on the specified surface and to maintain the states on the surface. However, chattering is the inherent phenomenon of SMC that cannot be ignored, which affects the control precision. To solve this problem, Gao et al. (2017) proposed a novel RBF based sliding mode controller, where an RBF neural network is employed to approximate the nonlinear uncertainties in the model. Levant (2005) presented a high order SMC to reduce the chattering problem and improve the convergence precision without knowing the accurate math model. In addition, a non-singular terminal sliding mode controller was used to overcome the shortcomings of slow convergence of traditional linear sliding mode (Feng et al., 2013). Li et al. (2011) proposed a dynamic optimal sliding-mode control to design the 6-DOF tracking control of both relative orbit and chaser attitude. A dynamic model of 6-DOF attitude-orbit coupling was established, and an integrated controller based on the traditional SMC method was designed (Sun et al., 2015; Zhang et al., 2015), in which an adaptive control law was used to estimate the parameters of the system. Motivated by the benefits of the SMC scheme and NNs, we consider to combine neural network and SM for control of the spacecraft control system.

The above-mentioned methods show benefits in coping with nonlinear systems control, but most of them have the following drawbacks: (i) The 6-DOF attitude-orbit synchronization motion model has uncertainty. (ii) The time-varying external disturbance and model uncertainty caused by accessories flexible vibration are not taken into account simultaneously, which is a problem for spacecraft control that cannot be ignored in practical applications. (iii) Most sliding mode controllers use a saturation function to suppress the chattering but this weakens robustness. Therefore, in order to implement the relative attitude and position control of the chaser approaching cooperative targets, model uncertainties, interference from the external space environment and the dithering in the traditional SMC should be addressed. This

2405-8963 Copyright © 2023 The Authors. This is an open access article under the CC BY-NC-ND license.
Peer review under responsibility of International Federation of Automatic Control.
10.1016/j.ifacol.2023.10.1223

work aims to tackle the above issues by combining SMC with neural network for the nonlinear control system of the spacecraft. The main contribution of this research is that a new adaptive sliding mode controller is designed to deal with the complex relative motion couplings, model uncertainty and external disturbance, in which adaptive estimation and compensation of system uncertainty and unknown time-varying external disturbance are achieved by using RBF neural network.

The remaining of the paper is organized as follows. Section 2 gives the 6-DoF spacecraft model and the control problem description. The robust controller combining SMC and RBFNN is developed and the stability analysis is provided in Section 3. Section 4 is a numerical example used to compare the proposed method with a standard SMC. Conclusions are given in Section 5.

2. MODELING AND PROBLEM DESCRIPTION

The tracking of the chaser to target spacecraft involves synchronous control of orbit and attitude. A 6-DOF relative dynamic model will be established, and an RBF neural network will be used to approximate the relative motion system and form an adaptive SMC strategy. The control block diagram of the system is shown in Fig. 1.

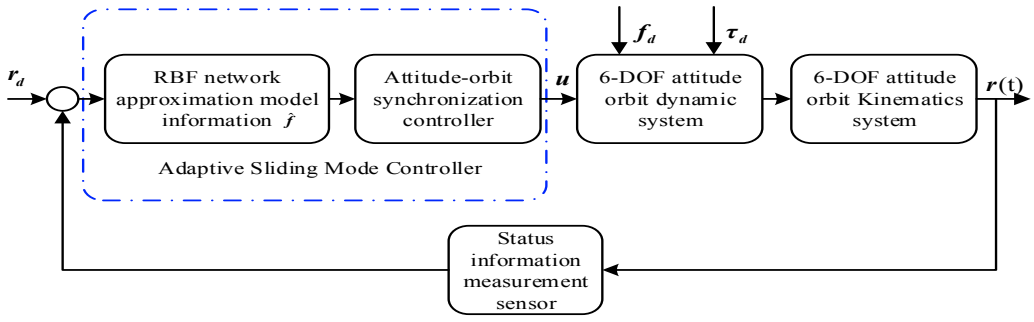

Fig. 1. Control block diagram of the system.

2.1 Relative Attitude Dynamics

For convenient analysis of the spatial angular position of a rigid body, take a point A on the rigid body, and the vector OA actually describes the spatial angular position of the rigid body. After time t, the position vector is at OA', as shown in Fig. 2.

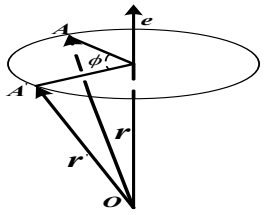

Fig. 2. Equivalent rotation of a rigid body.

According to Euler's theorem, the rotation of a rigid body from position A to A' can be equivalent to a single rotation ϕ around the axis e. Therefore, the modified Rodriguez parameters (MRPs) σ are defined as

$$\sigma = (\sigma_1, \sigma_2, \sigma_3)^T = \frac{esin\left(\frac{\phi}{2}\right)}{1+\cos\left(\frac{\phi}{2}\right)} = etan\frac{\phi}{4} \tag{1}$$

where $e = (e_1, e_2, e_3)^T$ is the unit vector of the Euler axis, and ϕ is the rotation angle of the Euler axis.

Suppose the chaser and target spacecraft are both rigid bodies, the attitude of spacecraft will be described by (1). When the rotation angle of equivalent rotation vector is $\phi \to \pm 360°$, there is $\tan\frac{\phi}{4} \to \infty$, MRPs are singular when $\phi = \pm 360°$. Therefore, MRPs can describe arbitrary posture rotation except for one full-circle attitude rotation. If the rotation angle is extremely small, the MRPs can be linearized to $\sigma \approx \frac{\phi}{4}e$ The coordinate transformation matrix C_{ct} of the chaser spacecraft body frame F_C to the reference frame F_T is

$$C_{ct} = I_3 + \frac{8S(\sigma)^2 - 4(1-\sigma^T\sigma)S(\sigma)}{(1+\sigma^T\sigma)^2} \tag{2}$$

where $S(\sigma)$ is the antisymmetric matrix, which is given by

$$S(\sigma) = \begin{bmatrix} 0 & -\sigma_3 & \sigma_2 \\ -\sigma_3 & 0 & -\sigma_1 \\ \sigma_2 & -\sigma_1 & 0 \end{bmatrix}$$

The attitude kinematics equation is described by MRPs as

$$\dot{\sigma} = Z(\sigma)\omega \tag{3}$$

where $\omega = (\omega_i, \omega_j, \omega_k)$ is the projection of the angular velocity of F_T relative to the F_O frame, and

$$Z(\sigma) = \frac{1}{4}[(1-\sigma^T\sigma)I_3 + 2\sigma\sigma^T + 2S(\sigma)] \tag{4}$$

where $\sigma = \sqrt{\sigma_1^2 + \sigma_2^2 + \sigma_3^2}$. Then

$$Z^T(\sigma)Z(\sigma) = \frac{1}{16}[(1-\sigma^T\sigma)^2 I_3 - 4S^2(\sigma) + 4\sigma\sigma^T] \tag{5}$$

where $S^2(\sigma) = \sigma\sigma^T - \sigma^T\sigma I_3$. The relative attitude angular velocity of the chaser and target spacecraft is expressed in frame F_C as

$$\omega_{ct} = \omega_c - C_{ct}\omega_t \tag{6}$$

Therefore, the spacecraft relative attitude dynamics model can be described as

$$\left.\begin{aligned} J\dot{\omega}_{ct} - J\omega_{ct}^{\times}\omega_{ct} &= \tau + \tau_d \\ \omega_{ct} &= \tfrac{16}{(1+\sigma^2)^2} Z^T(\sigma)\dot{\sigma} \end{aligned}\right\} \tag{7}$$

and the spacecraft relative attitude kinematic equation is

$$\dot{\sigma} = \tfrac{1}{2}(-\omega_{ct}^{\times} + \omega_{ct}\sigma\mathrm{I})\sigma + \tfrac{1}{4}\omega_{ct}(1-\sigma^2) \tag{8}$$

where J is the moment of inertia of the spacecraft and is positively symmetric, τ_d and τ are the disturbance torque and control torque acting on the spacecraft, respectively. Apply derivate to (3) and multiply it by $Z^{-T}JZ^{-1}$, and substituting $\omega = Z^{-1}(\sigma)\dot{\sigma}$ into (6), the spacecraft relative attitude dynamics model can also be described as

$$M_\sigma(\sigma)\ddot{\sigma} + C_\sigma(\sigma,\dot{\sigma})\dot{\sigma} = Z^{-T}(\sigma)(\tau + \tau_d) \tag{9}$$

where $M_\sigma = Z^{-T}(\sigma)JZ^{-1}(\sigma)$ is an asymmetric positive definite matrix, and $C_\sigma = -Z^{-T}(\sigma)JZ^{-1}(\sigma)\dot{Z}(\sigma)Z^{-1}(\sigma) - Z^{-T}(\sigma)S(JZ^{-1}(\sigma)\dot{\sigma})Z^{-1}(\sigma)$ is an antisymmetric matrix.

2.2 Relative Position Dynamics

Supposing the virtual reference spacecraft is traveling on a circular orbit that is not affected by perturbation, the dynamics of the target spacecraft and the tracking spacecraft are written as (10) and (11), respectively.

$$\frac{d^2 r_t}{dt^2} = -\frac{\mu}{r_t^3} r_t + a_t + \frac{f_{td}}{m} \tag{10}$$

$$\frac{d^2 r_c}{dt^2} = -\frac{\mu}{r_c^3} r_c + a_c + \frac{f_{cd}}{m} \tag{11}$$

where $\mu = 3.986005 \times 10^{14} m^3/s^2$ is the earth's gravity constant, a_t, a_c represent the acceleration of the target spacecraft and tracking spacecraft, respectively. $\frac{f_{td}}{m}$ and $\frac{f_{cd}}{m}$ are the disturbance acceleration of the target spacecraft and tracking spacecraft, respectively.

Defining the relative position vector from target to chaser as $q = r_c - r_t = [x \quad y \quad z]^T$, represented in the target satellite orbit frame, the relative motion dynamics is governed by

$$\frac{d^2 q}{dt^2} = -\frac{\mu}{r_t^3} r_t + \frac{\mu}{r_t^3} r_c + a_t - a_c + \left(\frac{f_{td} - f_{cd}}{m}\right) \tag{12}$$

When the target spacecraft has no autonomous acceleration, i.e., $a_t = 0$, the projection in the target spacecraft's dynamic coordinate system is

$$\begin{aligned} \frac{d^2 q}{dt^2} + [\dot{\omega}_\times]q + 2[\omega_\times]\frac{dq}{dt} + [\omega_\times][\omega_\times]q = \\ -a_c + \left(-\frac{u}{r_t^3} r_t + \frac{u}{r_c^3} r_c\right) + \left(\frac{f_{td} - f_{cd}}{m}\right) \end{aligned} \tag{13}$$

where $\omega = [\omega_i \quad \omega_j \quad \omega_k]^T$ represents the orbital angular velocity of the target spacecraft, and

$$[\omega_\times] = S(\omega) = \begin{bmatrix} 0 & -\omega_k & \omega_j \\ \omega_k & 0 & -\omega_i \\ -\omega_j & \omega_i & 0 \end{bmatrix}.$$

Equation (13) can be written as

$$M_x\ddot{q} + C_x\dot{q} + D_x q = f + f_d \tag{14}$$

where $M_x = mI_3$, $C_x = 2mS(\omega)$,

$$D_X = m\begin{bmatrix} -\omega_j^2 - \omega_k^2 & \omega_i\omega_j & \omega_i\omega_k \\ \omega_i\omega_j & -\omega_i^2 - \omega_k^2 & \omega_j\omega_k \\ \omega_i\omega_k & \omega_j\omega_k & -\omega_i^2 - \omega_j^2 \end{bmatrix} + mS(\dot{\omega}),$$

f and $f_d = f_{td} - f_{cd}$ are the control force and disturbance force of the chaser. The effect of attitude on the orbit is reflected in the matrix C_x and D_x. Therefore, the relative attitude dynamics and the orbital dynamics are coupled.

2.3 Integrated Relative Motion Dynamics

Denote $r = [\sigma^T, q^T]^T$ as the state variable of the spacecraft. The dynamics of the two motions need to be expressed in a unified representation, and the dynamics for relative position and attitude between the chaser spacecraft and the target spacecraft can be expressed as

$$M\ddot{r} + C\dot{r} + G(r) = u + u_d \tag{15}$$

where $M = \begin{bmatrix} M_\sigma & 0_{3\times3} \\ 0_{3\times3} & M_x \end{bmatrix}$ is a symmetric positive definite matrix, $C = \begin{bmatrix} C_\sigma & 0_{3\times3} \\ 0_{3\times3} & C_x \end{bmatrix}$ is a Coriolis force and centrifugal force matrix, $G = \begin{bmatrix} 0_{3\times1} \\ D(r) \end{bmatrix}$ inertia vector, $u = \begin{bmatrix} Z^{-T}(\sigma) \\ f \end{bmatrix}$ the control input, and $u_d = \begin{bmatrix} \tau_d \\ f_d \end{bmatrix}$ disturbance.

In the system model (15), for the chaser mass *m*, inertia matrix J, external disturbance force f_d, disturbance torque τ_d, and target orbital elements, the following assumptions are made in the subsequent development in this paper.

Assumption 1 The chaser mass m is a positive scalar and is constant. In the autonomous proximity phase, the spacecraft relative distance is small, and the loss massed by burning fuel is small relative to the total mass, thus can be ignored. The inertia matrix J is a symmetric positive definite matrix, and the external disturbance torques and forces are continuously differentiable and bounded.

Assumption 2 The target spacecraft does not have orbital maneuvers, and the travel on classical Kepler orbits and the orbital parameters are known.

Assumption 3 The spacecraft's orbit is safe and reliable, and there is no space debris and other trash. As a result, there's no need to consider collision avoidance in this study. The relative position and relative velocity of the chaser can be directly measured.

The control objectives are on the relative position and attitude of the two spacecrafts. It is required that the relative position error $q_e = 0$ and the relative velocity error $\dot{q}_e = 0$ gradually, simultaneously, and the attitude error $\sigma_e = 0$ and the angular velocity error $\dot{\sigma}_e = 0$, respectively. Therefore, the control objective in this work is equivalent to designing a controller to guarantee $\lim_{t\to\infty} r(t) = 0$.

3. CONTROLLER DESIGN AND STABILITY ANALYSIS

3.1 Sliding Mode Surface

For a nonlinear system

$$\dot{x}(t) = f(x,t) \tag{16}$$

there is a super surface called sliding mode surface, $s = 0$, that divides the state space of the system into two parts, $s < 0$ and $s > 0$. The point movement of the system on the sliding mode surface can be classified into three cases and the movement characteristics on the sliding surface are shown in Fig. 3.

When a point on the system moves near the sliding mode surface $s = 0$, if the point passes through point A, the point is called the normal point; if the point leaves point B from both sides near the sliding surface, the point is called the starting point; If the point gradually approaches point C from both sides, the point is called the endpoint.

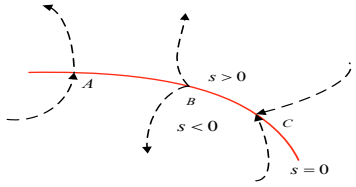

Fig. 3. Movement characteristics of points on the sliding surface

If all the points on the sliding modal area become endpoints, there will be

$$\lim_{s\to 0} s\dot{s} \le 0 \tag{17}$$

This means that there is a non-increasing function in the vicinity, so the system will also be stable on the sliding mode surface.

3.2 RBFNN-SM Controller Design

Define tracking error vector $e(t) = r_d(t) - r(t)$ and design the sliding mode function

$$g = \dot{e} + \Lambda e = \dot{r}_d - \dot{r} + \Lambda e \tag{18}$$

where $\Lambda = [\lambda_1 \quad \lambda_2 \quad \dots \quad \lambda_n]^T > 0$, and ensure $s^{n-1} + \lambda_{n-1}s^{n-2} + \cdots + \lambda_1$ is Hurwitz, that is, when $r \to 0$, $e \to 0$, then $\dot{r} = -g + \dot{r}_d + \Lambda e$, and

$$\begin{aligned} M\dot{g} &= M(\ddot{r}_d - \ddot{r} + \Lambda\dot{e}) = M(\ddot{r}_d + \Lambda\dot{e}) - M\ddot{r} \\ &= M(\ddot{r}_d + \Lambda\dot{e}) + C\dot{r} + G + u_d - u = -Cg - u + f \end{aligned} \tag{19}$$

where $f = M\ddot{r}_f + C\dot{r}_f + G + u_d$, $\dot{r}_f = \dot{r}_d + \Lambda e$, and the expression f contains all the information in the model. Therefore, the control objectives can be approximated by the RBF neural network, and a robust controller that does not accurately require model information can be designed.

A RBFNN is a type of feed forward neural network composed of three layers, namely the input layer, the hidden layer and the output layer. Approaching the output $f(x)$ with RBF network, the algorithm is described as

$$f(x) = W^T h + \varepsilon \tag{20}$$

Define the approximation term $\hat{f} = \hat{W}^T h$, therefore

$$f - \hat{f} = W^T h + \varepsilon - \hat{W}^T h = \tilde{W}^T h + \varepsilon \tag{21}$$

where x is the input of RBFNN, W is the ideal weight matrix, ε is a minimal positive real scalar, h is the Gaussian function and $h_j = exp\left\{\frac{(x-\mu_j)^2}{\sigma_j^2}\right\}$, $\tilde{W} = W - \hat{W}$, $\|W\|_F = W_{max}$.

According to the design method in (Liu et al., 2010), the control law of the spacecraft attitude orbit coupling system can be designed as

$$u = \hat{f} + K_v g - \varsigma \tag{22}$$

where $\varsigma = -(\varepsilon_N + b_d)sgn(g)$ is a term for robustness. The RBF network weight adaptive law is defined as

$$\dot{\hat{W}} = \Gamma h g^T \tag{23}$$

where $\Gamma = \Gamma^T > 0$. Substituting robust adaptive controller (22) into (19) yields

$$\begin{aligned} M\dot{g} &= -Cg - \left[\hat{f} + K_v\sigma - \varsigma\right] + f + u_d \\ &= -(K_v + C)g + \tilde{W}^T h + (\varepsilon + u_d) + \varsigma \end{aligned} \tag{24}$$

3.3 Stability Analysis

Defining Lyapunov function L, the stability property of the system is found using the function

$$L = \frac{1}{2}g^T M g + \frac{1}{2}tr\left(\tilde{W}^T\Gamma^{-1}\tilde{W}\right) \tag{25}$$

where $tr(\cdot)$ represents the trace of the matrix. The derivative of (25) is computed, and substituting (24) into it gives

$$\begin{aligned} \dot{L} &= g^T M\dot{g} + \frac{1}{2}g^T\dot{M}g + tr\left(\tilde{W}^T\Gamma^{-1}\dot{\tilde{W}}\right) \\ &= g^T\left[-(K_v + C)g + \tilde{W}^T h + (\varepsilon + u_d) + \varsigma\right] + \\ &\quad \frac{1}{2}g^T\dot{M}g + tr\left(\tilde{W}^T\Gamma^{-1}\dot{\tilde{W}}\right) \\ &= -g^T K_v g + \frac{1}{2}g^T(\dot{M} - 2C)g + tr\left(\tilde{W}^T\Gamma^{-1}\dot{\tilde{W}}\right) + \\ &\quad g^T\tilde{W}^T h + g^T(\varepsilon + u_d + \varsigma) \end{aligned} \tag{26}$$

According to the following characteristics (Broomhead et al.,1988):

1) Skew symmetry of the dynamic model $g^T(M - 2C)g = 0$,

2) $\dot{\tilde{W}} = -\dot{\hat{W}} = -\Gamma h g^T$,

3) $g^T\tilde{W}^T h = tr\left(\tilde{W}^T h g^T\right)$,

Equation (26) can be written as

$$\dot{L} = -g^T K_v g + g^T(\varepsilon + u_d + \varsigma) \tag{27}$$

In addition,

$$\begin{aligned} &g^{\mathrm{T}}(\varepsilon + u_d + \varsigma) \\ &= g^{\mathrm{T}}(\varepsilon + u_d) + g^{\mathrm{T}}\left(-(\varepsilon_N - b_d)sgn(g)\right) \\ &= g^{\mathrm{T}}(\varepsilon + u_d) - \|g\|(\varepsilon_N - b_d) \le 0 \end{aligned} \tag{28}$$

hence

$$\dot{L} \le -g^T K_v g \le 0.$$

As $L \ge 0$, $\dot{L} \le 0$, g and $\widetilde{W}$ are bounded. When $\dot{L} \equiv 0$, it is known that $g = 0$. Additionally, when $t \to \infty$, $g \to \infty$, thereby $e \to 0$ and $\dot{e} \to 0$. Therefore, the closed-loop system is progressively stable.

4. NUMERICAL EXAMPLE

An example of a close proximity mission in orbit is simulated in this section. The target spacecraft's orbit elements are: $a = 6900km$, $e = 0.005$, $i = 100°$, $\Omega = 70°$, $\omega = 30°$, $f = 0°$. The initial relative position and attitude are consistent with those in (Liu et al., 2016), with the specific values given in Table 1. The expected relative position x_d, velocity $\dot{x}_d$, attitude angle σ_d and attitude angular velocity $\dot{\sigma}_d$ are set to zero, respectively.

The chaser's disturbance force and torque are written as
$f_d = [10^{-3} \times [2.5 \quad 4.5 \quad 3.6]^T + N(0, \upsilon_P)] * m,$

$$\tau_d = \begin{bmatrix} A_0(3\cos(\omega_0 t + 1)) \\ A_0(1.5\sin(\omega_0 t) + 3\cos(\omega_0 t)) \\ A_0(3\sin(\omega_0 t) + 1) \end{bmatrix} + N(0, \upsilon_\sigma),$$

The chaser's disturbance force and torque are written as
$f_d = [10^{-3} \times [2.5 \quad 4.5 \quad 3.6]^T + N(0, \upsilon_P)] * m,$

$$\tau_d = \begin{bmatrix} A_0(3\cos(\omega_0 t + 1)) \\ A_0(1.5\sin(\omega_0 t) + 3\cos(\omega_0 t)) \\ A_0(3\sin(\omega_0 t) + 1) \end{bmatrix} + N(0, \upsilon_\sigma),$$

where the spacecraft mass is $m = 50kg$, $A_0 = 1.5 \times 10^{-3} N \cdot m$, ω_0 is the orbital angular velocity, $N(0, \upsilon)$ is the Gaussian noise, $\upsilon_P = 10^{-3}$, $\upsilon_\sigma = 10^{-3}$. Additionally, the RBF neural network structure takes nodes of 6-7-1 in the three layers. The initial weight is 0, and the Gaussian function parameters are $b_i = 0.02$, $K_v = 2 * diag(1,1,1,1,1,1)$, c_i = [-0.001 -0.001 -0.001 0 0.001 0.001 0.001], $\varepsilon_v = 0.001$, and $b_d = 0.04$, respectively.

Table 1. Simulation parameters

Parameter	Value
$J(kg \cdot m^2)$	$diag(8.0 \quad 6.0 \quad 11.5)$
$x_0(m)$	$[-8.68 \quad 4.04 \quad 2.88]^T$
$\dot{x}_0(m/s)$	$[-0.15 \quad 0.2 \quad -0.1]^T$
$\sigma_0(rad)$	$[-0.362 \quad 0.291 \quad -0.155]^T$
$\dot{\sigma}_0(rad/s)$	$[-0.11 \quad 0.056 \quad 0.011]^T$

The proposed RBFNN-based SM controller is compared with the second-order terminal sliding mode controller in (Liu et al., 2016) to verify the controller's dynamic characteristics, steady-state response, and robustness. To make a more intuitive comparison of the two controllers, and adjust the convergence time to a similar range, the relative position curves of the two controllers, RBF-SM and SM, are shown in Fig. 4 and Fig. 5, respectively.

Both methods can control the spacecraft to achieve the desired position for a limited time. However, compared with the SM controller, the RBF-SM controller has higher control precision. The root mean square error (RMSE) of the position accuracy of RBF-SM and SM within 190-200 seconds are 0.00025m and 0.0072m, respectively, and the relative position control accuracy 10^{-4} and 10^{-3} magnitude, respectively. The zoomed part of the picture shows that the RBF-SM controller has less chatter than the SM controller in the last ten seconds.

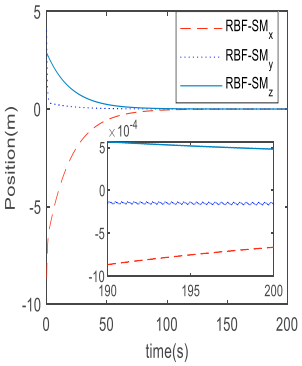

Fig. 4. RBF-SM relative position response curve.

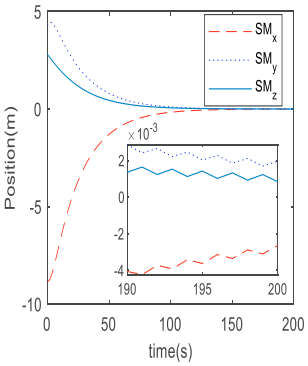

Fig. 5. SM relative position response curve.

The relative attitude angle curves under the two controllers are shown in Fig. 6 and Fig. 7. Both methods can control the chaser to achieve the desired target state. However, compared with the SM controller, the proposed RBF-SM controller again has higher control precision; the RMSE for the last 10 seconds of relative attitude control can reach $2.59 \times 10^{-7} rad$, while the SM controller's RMSE is $1.52 \times 10^{-5} rad$.

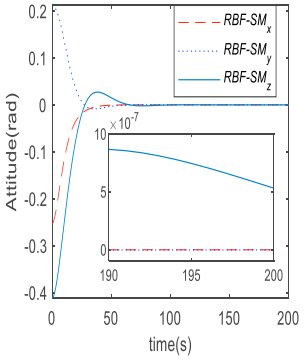

Fig. 6. RBF-SM relative attitude angle response

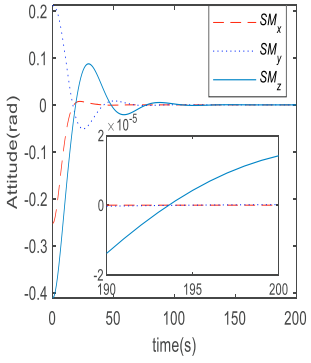

Fig. 7. SM relative attitude angle response curve.

The relative position and relative attitude comparison curves are shown in Fig. 8 and Fig. 9, respectively. As shown in Fig. 8, the relative position motion of the RBF-SM controller converges faster than the SM controller, especially on the y-axis, because the relative positional motion is not coupled to the orbital plane on $S_R - xz$ in the y-axis. Fig. 9 shows that RBF-SMC is more advantageous than SMC for the attitude angle convergence speed, reaching the desired state value at about 110s, and the overshoot is stay within 20%.

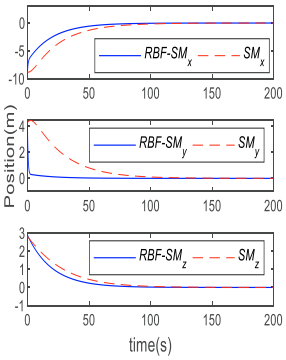

Fig. 8. Relative position.

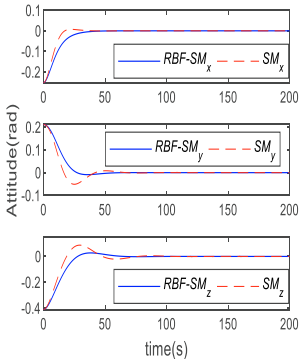

Fig. 9. Relative attitude.

The control force and control torque comparison curves are shown in Fig. 10 and Fig. 11. In order to more clearly observe the characteristics of the control force, Fig. 10 only shows the data for the first 100 seconds, which exhibits no chattering phenomenon in RBF-SM relative to SM. As shown in Fig. 11, the RBF-SM controller has a smaller overshoot in control torques.

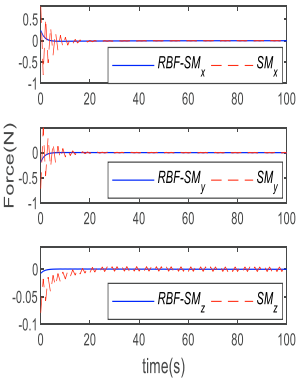

Fig. 10. Control force.

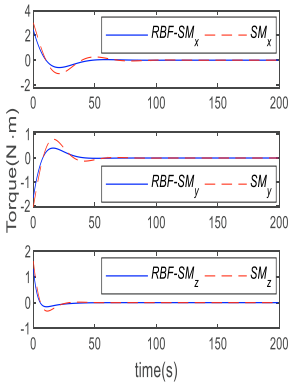

Fig. 11. Control torque.

5. CONCLUSIONS

The control of the relative position and attitude of the spacecraft without maneuver is investigated in this work. A 6-DOF relative motion model in reference orbit frame is established firstly, and the MRPs are used to describe the attitude rotation to reduce the singularity. Based on the relative position and relative attitude dynamics model, a robust adaptive RBFNN-based SMC has been developed. The closed-loop system performance is verified by numerical simulation. The results show that the proposed controller can successfully attenuate the attitude and position error, weaken the chattering in control force and decrease the overshoot of the control torque. In future works, the proposed controller will be further developed to consider constraints on actuators and specific space mission requirements in operation.

ACKNOWLEDGEMENT

This work is supported by the National Natural Science Foundation of China (No. 72071183), the Opening Foundation of Shanxi Key Laboratory of High Performance Battery Materials and Devices (No. 2022HPBMD01002), and the Research Project Supported by Shanxi Scholarship Council of China (No.2020-114).

REFERENCES

Broomhead, D. and Lowe, D. (1988). Multivariable Functional Interpolation and Adaptive Networks. *Complex Systems*, 2(3), 321-355.

Feng, Y., Yu, X.H., and Han, F.L. (2013). On nonsingular terminal sliding mode Control of nonlinear systems. *Automatica*, 49(6), 1715-1722.

Gao, W., Shi, J.B., Wang, W.Q., and Sun, Y. (2017). Research on sliding mode control for robotic manipulator based on RBF neural network. *The 29th Chinese Control and Decision Conference (CCDC)*, 4934-4938.

Ge, S.S., Hang, C.C., Lee, T.H., and Zhang, T. (2010). Stable Adaptive Neural Network Control. Springer Publishing Company, New York, United States.

Kong, X.R., Yang, Z.X., Liao, J., and Zhang, Y.C. (2011). Adaptive multilayer neural network tracking control for flexible spacecraft. *Systems Engineering and Electronics*, 33(9), 2039-2044.

Levant, A. (2005). Homogeneity approach to high-order sliding mode design. *Automatica*, 41(5), 823-830.

Levin, A.U. and Narendra, K.S. (1996). Control of nonlinear dynamical systems using neural networks-Part II: Observability identification and control. *IEEE Transactions on Neural Networks*, 7(1), 30-42.

Lewis, F.L., Yesildirek, A., and Jagannathan, S. (1998). Neural Network Control of Robot Manipulators and Nonlinear Systems. Taylor & Francis, Philadelphia, United States.

Li, Y.K., Jing, Z.L., and Hu, S.Q. (2011). Dynamic optimal sliding-mode control for six-DOF follow-up robust tracking of active satellite. *Acta Astronautica*, 69(7-8), 559-570.

Liu, H.L., Shi. X.P., Zhang, J., and Bi, X.T. (2016). Adaptive second order terminal sliding mode control for approach to non-cooperative target. *Systems Engineering and Electronics*, 38(10), 2353-2360.

Liu, J.K. and Lu, Y. (2010). Adaptive RBF neural network control of robot with actuator nonlinearities. *Journal of Control Theory and Applications*, 8(2), 249-256.

Narendra, K.S. and Parthasarathy, K. (1990). Identification and control of dynamic systems using neural networks. *IEEE Transactions on Neural Networks*, 1(1), 4-27.

Sun, L. and Huo, W. (2015). Robust adaptive relative position tracking and attitude synchronization for spacecraft rendezvous. *Aerospace Science and Technology*, 41, 28-35.

Wang, H., Kong, H., and Yu, M. (2015). RBF-neural-network-based sliding mode controller of automotive Steer-by-Wire systems. *International Conference on Natural Computation (ICNC)*, 907-914.

Yuan, C.Q., Li, Z.G., Yu, H.L., and Zuo, C.Y. (2019). Robust attitude tracking control of multi spacecraft based on RBF neural network. *Aerospace Control and Application*, 45(3), 39-43,52.

Zhang, Q.Z., Jin, Y.Q., Kang, Z.Y.， and Xiao， Y.Z.(2015). Coupled control of relative position and attitude for servicing spacecraft approaching the target in close proximity. *Systems Engineering and Electronics*, 37(1), 141-147.